Molecular Dynamics Simulations

International Edition: DOI: 10.1002/anie.201913257
German Edition: DOI: 10.1002/ange.201913257

Atomistic Simulations of COSAN: Amphiphiles without a Head-and-Tail Design Display "Head and Tail" Surfactant Behavior

David C. Malaspina, Clara Viñas, Francesc Teixidor, and Jordi Faraudo**

Abstract: *Cobaltabisdicarbollide (COSAN) anions have an unexpectedly rich self-assembly behavior, which can lead to vesicles and micelles without having a classical surfactant molecular architecture. This was rationalized by the introduction of new terminology and novel driving forces. A key aspect in the interpretation of COSAN behavior is the assumption that the most stable form of these ions is the transoid rotamer, which lacks a "hydrophilic head" and a "hydrophobic tail". Using implicit solvent DFT calculations and MD simulations we show that in water, 1) the cisoid rotamer is the most stable form of COSAN and 2) this cisoid rotamer has a well-defined hydrophilic polar region ("head") and a hydrophobic apolar region ("tail"). In addition, our simulations show that the properties of this rotamer in water (interfacial affinity, micellization) match those expected for a classical surfactant. Therefore, we conclude that the experimental results for the COSAN ions can now be understood in terms of its amphiphilic molecular architecture.*

Surfactants are molecules that alter the surface tension between two phases, commonly one being water whereas the second is air or oil.[1] To achieve this surfactants are structurally amphiphilic, made of a polar side and a non-polar side. The first is hydrophilic whereas the second is lipophilic. The non-polar side is similar in most surfactants and is usually made of a long hydrocarbon tail and a small polar head, such as sulphate, sulphonate, carboxylate or a quaternary ammonium as the most popular heads. Besides modifying the surface tension, surfactants form aggregates, such as micelles, vesicles, rods or lipid bilayers in the bulk aqueous phase. The shape of the aggregates depends on the chemical structure of the surfactants, namely the balance in size between the hydrophilic head and hydrophobic tail.[1–3] This short description of surfactants provides an easy structure–activity connection. However, certain anions of nanometric size (cobaltabisdicarbollide $[Co(C_2B_9H_{11})_2]^-$ known as COSAN, see Figure 1) have been recently reported to self-assemble in bulk water to produce vesicles and micelles, behavior typical of surfactants.[4–7] As can be seen in Figure 1, there is neither a hydrocarbon chain as a hydrophobic tail nor a polar group as a headgroup like in a conventional surfactant, so the structure–activity connection is not obvious. For this reason, new concepts, such as theta-shaped amphiphile,[4] stealth amphiphile[7,8] and intrinsic amphiphile,[9] were coined to describe this novel amphiphilic behavior.

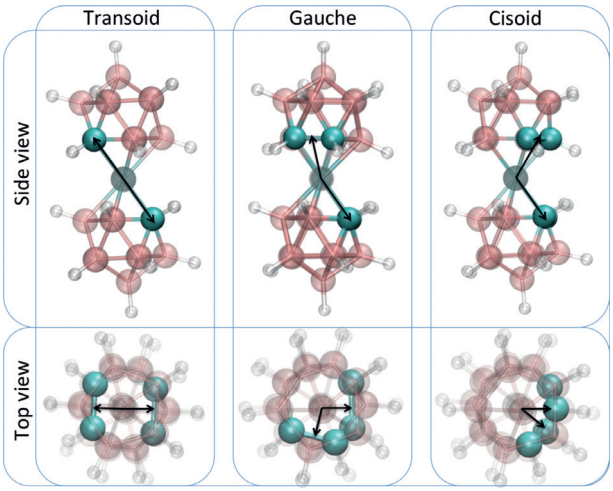

Figure 1. Top and side views of the atomic structure of the cobaltabisdicarbollide $[Co(C_2B_9H_{11})_2]^-$ (COSAN) anion in its three rotameric forms (*cis*-, *gauche*- and *trans*-). C cyan, H white, B orange, Co gray.

The detailed molecular mechanism underlying this non-classical amphiphilic behavior is still unknown. Some proposals emphasize the possibility of a non-classical hydrophobic effect[7,9,10] or a so-called chaotropic effect[7,11] as a driving force for the association of COSAN in water, intrinsically different from the association mechanism of classical surfactants.

However, it is also known[12] that one of the specific rotameric forms of COSAN (the *cisoid* rotamer, see Figure 1) has a charge distribution resembling that of an anionic surfactant, with a polar region (concentrating most of the anion charge) and an apolar region. Another key aspect is that small changes in the structure of COSAN that block particular rotameric forms lead to different self-assembled structures.[13] This observation led us to consider whether there could be an explanation for the observed behavior of COSAN in terms of its molecular architecture similarly to classical surfactants, a goal that we have accomplished here by combining DFT calculations in implicit solvent and MD simulations in explicit solvent.

A key feature in the COSAN anion is that the B–H/C–H bonds tilt away from the C_2B_3 layer towards the metal that prevents free rotation,[14] thus producing three main rotameric

[*] Dr. D. C. Malaspina, Prof. Dr. C. Viñas, Prof. Dr. F. Teixidor, Dr. J. Faraudo
Institut de Ciència de Materials de Barcelona, ICMAB-CSIC
Campus de la UAB, 08193 Bellaterra (Spain)
E-mail: teixidor@icmab.es
jfaraudo@icmab.es

Supporting information and the ORCID identification number(s) for the author(s) of this article can be found under: https://doi.org/10.1002/anie.201913257.

forms of different energy, as shown in Figure 1, in which the *cis* and *gauche* rotamers are able to have clockwise and counterclockwise forms. The *transoid* rotamer is the one with lower energy "in vacuo", as shown by quantum chemical calculations.[15,16] However, a previous study conducted by some of us[12] found that this rotamer is only present at about 8% in crystal structures with the composition M[Co-$(C_2B_9H_{11})_2$]. Largely, the most abundant rotamer in the solid state is the *cis* rotamer (Table 1). In addition, DFT calculations in crystals[12] reveal that *cis*-COSAN is the most stable rotamer due to molecule–molecule interactions. This confirms the impact of the interactions with the molecule environment on the stability of the COSAN structure.

Table 1: Results for DFT calculations of the COSAN rotamers shown in Figure 1.[a]

	Transoid	*Gauche*	*Cisoid*
ΔE in vacuo [kJ mol^{-1}]	0.0	3.40	14.7
ΔE in water [kJ mol^{-1}]	0.0	−3.67	−8.36
Population in solution (water at 298 K)	1.4%	12.8%	85.8%
Crystal population[12]	8.2%	15.6%	76.2%

[a] ΔE is the energy difference of each rotamer (in kJ mol^{-1}) with *trans*-COSAN, calculated by DFT methods both in vacuo and in water (see text). The population % of each isomer in water at 298 K is calculated from ΔE using the Boltzmann thermodynamic equilibrium distribution (see Supporting Information). The population % of each rotamer in the solid state was determined from the CSD crystal database in Ref. [12].

Among the factors that appear to be involved in the preferred solid state conformation for $[Co(C_2B_9H_{11})_2]^-$ is the ability of the C_c-H protons to produce a high number of C_c–H···H–B interactions,[12] which remarkably are only observed in *cisoid* conformations. The ability to produce C_c–H···H–B interactions in the solid state was associated with the higher prevalence of the *cis* rotamer. Indeed, the *trans* isomer was incapable of producing such interactions, which explains its low abundance. We suspected that this impact of the immediate surrounding over COSAN could also be applicable in water solution, and that the interactions of a particular rotamer with water could explain the apparently non-classical amphiphilic behavior of these molecules.

For this reason, we have performed DFT calculations using Gaussian 16[17] at the B3LYP/6-31G* level of theory[18,19] both in vacuo and in presence of implicit water solvent.[20,21] The effect of water was modelled using the integral equation formalism variant of the polarizable continuum model (IEFPCM)[21,22] (see details in the Supporting Information). Remarkably, our results (Table 1) demonstrate that water stabilizes the *cisoid* rotamer. Assuming a thermodynamic equilibrium in water, the distribution population of rotamers will be largely dominated by the *cisoid* rotamer, as shown in Table 1. It is worth noting the similarities in the population of the different rotamers obtained in our predictions for COSAN ions in water and the experimental data from crystal structures. Our result highlights that calculations of molecules in vacuo could be highly misleading when they are used to analyze the condensed phase.

The particular geometry of the *cisoid* rotamer, as shown in Figure 1, defines two distinct regions in the molecule, one delimited by the boron atoms and the other one delimited by the carbon atoms. These two regions have different electronic properties. As shown in Figure 7 of Ref. [12], the region delimited by the carbon atoms has a low charge density, whereas the boron atoms geometrically opposed to this region concentrate the negative charge of the anion. This molecular architecture strongly suggests that *cis*-COSAN could be a surfactant with the four carbon atoms delimiting the hydrophobic region of the molecule since it is the low charge density region of the molecule. The boron atoms with high charge density will correspond to the hydrophilic regions of the molecule. This concept was proved by performing a series of all-atomic molecular dynamics (MD) simulations[20] of *cis*-COSAN in water using the NAMD[24] program and a CHARMM36-compatible force field[25–27] (see details in the Supporting Information).

We first considered a *cis*-COSAN anion with a Na^+ counterion in a water/vacuum slab. In our simulations, the *cis*-COSAN anion adsorbs spontaneously at the water interface, with the preferred orientation shown in Figure 2a (see the full statistical analysis of *cis*-COSAN orientation in the Supporting Information). In this orientation, the four carbon atoms delimiting the hydrophobic region of the molecule are located away from water and the boron atoms corresponding to the hydrophilic regions of the molecule are oriented towards water. Another simple way to identify hydrophobic and hydrophilic regions is to perform biased MD simulations in which the *cis*-COSAN molecule is slowly pulled from its equilibrium position at the interface away from the water phase, towards the vacuum. As can be seen in Figure 2b,c, the region of the *cis*-COSAN anion identified as hydrophilic retained the hydration water during the pulling process. This behavior is equivalent to that observed in our previous simulations[28] of classical surfactants at a water/vacuum interface (see the comparison in Figure S2).

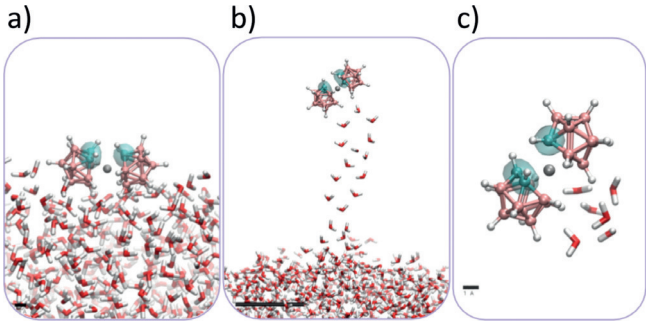

Figure 2. Snapshots from MD simulations of *cis*-COSAN at 298 K at a water/vacuum interface. a) Snapshot showing the preferred orientation in equilibrium simulations. b, c) Biased MD-simulations in which the *cis*-COSAN molecule is slowly pulled from the interface. Water molecules are shown in licorice representation and the *cis*-COSAN anion is shown in CPK representation with the central Co atom in gray. The carbon atoms from the proposed hydrophobic regions of *cis*-COSAN are highlighted in cyan. All images were made using VMD.[23] The bar scale corresponds to 1 nm for (a) and (b) and to 1 Å for (c).

Therefore, the MD simulations predict that *cis*-COSAN is a surfactant molecule since it adsorbs at a water interface. We next wanted to show that simulations predict an interface activity for *cis*-COSAN as strong as that of classical ionic surfactants with long hydrocarbon chains. To this end, we have performed additional biased ABF-MD simulations[29] at 298 K, in which a *cis*-COSAN anion and a Na^+ counterion were initially placed in vacuum, thermalized, and slowly transferred to the water phase. The obtained free-energy profile is shown in Figure 3. We also show results for the same

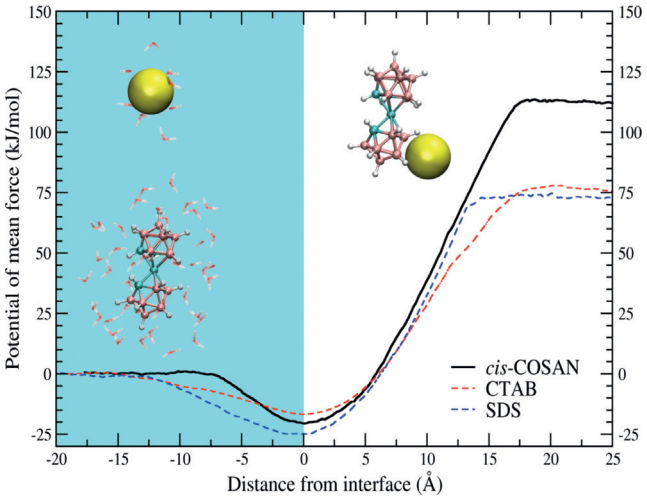

Figure 3. Results from ABF-MD simulations of a *cis*-COSAN anion at a water/vacuum interface. The origin of the free energy (potential of mean force) is taken at the water phase and the origin of abscissas is taken at the equilibrium position of *cis*-COSAN at the water/vacuum interface. The shaded region corresponds to the water phase. (Snapshots illustrate typical configurations of *cis*-COSAN and Na^+ in each phase.) For comparison we also show the results of an analogous calculation for CTAB and SDS surfactants (see Supporting Information).

calculation with the classical surfactants anionic sodium dodecyl sulfate (SDS) and cationic cetyltrimethylammonium bromide (CTAB). As shown in Figure 3, the potential of mean force (free-energy profile) has the same shape for *cis*-COSAN, SDS, and CTAB. The value of the free-energy minima at the interface for *cis*-COSAN ($-20.5\ kJ\,mol^{-1}$) is of the same magnitude as the values found for classical surfactants, between the values obtained for CTAB and SDS. Figure 3 also shows that *cis*-COSAN has a larger solvation free energy (ca. $-110\ kJ\,mol^{-1}$) than SDS and CTAB. This is consistent with the fact that *cis*-COSAN has a large hydrophilic region and a small hydrophobic region, whereas CTAB and SDS have a small hydrophilic headgroup and a long apolar hydrocarbon tail.

A consequence of the amphiphilic nature of *cis*-COSAN predicted by the results of Figures 2 and 3 is that, in water solution and in the absence of an interface, we should expect a substantial self-assembly of *cis*-COSAN molecules (as for classical surfactants). In order to study the self-assembly behavior of *cis*-COSAN, we have performed extensive, large-scale atomistic MD simulations of COSAN in water at different concentrations (the simulations at the lowest concentration contain ca. 780000 atoms). The results, summarized in Figures 4, S6, and S7 (Supporting information), show a self-assembly to micelles which depends on the concentration of *cis*-COSAN.

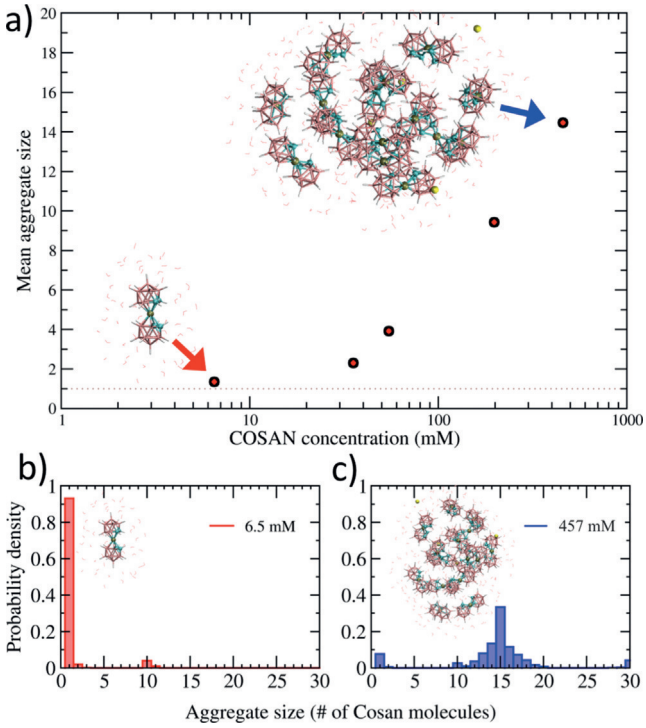

Figure 4. a) Average number of aggregates per micelle as computed in large-scale MD simulations. The arrows indicate the two simulations for which the detailed distribution is shown in panels (b) and (c). Bottom panels: Distribution of aggregate size of *cis*-COSAN obtained from MD simulations in water for two different *cis*-COSAN concentrations: 6.5 mM in panel (b) and 457 mM in panel (c). The inset in each panel shows a snapshot of the most probable aggregation state. The color scheme is the same as in Figures 2 and 3.

The average aggregation number as a function of concentration obtained from our MD simulations (Figure 4a) is consistent with the experimentally determined[6,7,10,13] critical aggregation concentration for micelles of Na^+COSAN^-, which is ca. 10 mM.

At the lowest simulated concentration (6.5 mM), almost all *cis*-COSAN are found not associated (as monomers in water) in equilibrium with a very small fraction of *cis*-COSAN associated in micelles (Figure 4b). As the concentration increases, the fraction of *cis*-COSAN in monomeric form rapidly decreases and micelles dominate. The micelles have a bell-shaped distribution of sizes with a well-defined peak, as shown in Figure 4c for a concentration of ca. 457 mM (see also Figure S4 for all concentrations). In this case, the peak corresponds to a micelle composed by 15 *cis*-COSAN, close to the experimental size reported in Ref. [4]. In addition, these experiments show a broad SWAXS peak at around $11\ nm^{-1}$, consistent with the Co–Co distance of ca. 7 Å between first-neighbor *cis*-COSAN molecules inside the micelle obtained in our simulations (see Supporting Informa-

tion). In fact, the internal structure of the micelles has a short-range order, as shown by the presence of two peaks (at ca. 7 and 8.7 Å) in the $g(r)$ function between Co atoms (see Figure S4). This short-range order is in contrast to the liquid structure usually found inside micelles of classical surfactants (such as CTAB or SDS), which is due to the flexibility of the alkyl chains. The orientation of *cis*-COSAN molecules inside the micelle is also interesting. The hydrophobic regions of the *cis*-COSAN molecules are oriented towards the interior of the micelles (see snapshots in Figures 4 and S4). Moreover, as shown in Figure S4, adjacent *cis*-COSAN molecules have a tendency to be in parallel orientation.

It should be noted that, experimentally, the micelles are observed to coexist with vesicles of ca. 20 nm in radius[4,6,10] with aggregation numbers of about 12500 molecules.[4] Attempts to directly simulate these vesicles in water require the use of coarse-grain models instead of the all-atomic MD simulations discussed here. However, the ordering of *cis*-COSAN molecules in the vesicle walls can be analyzed by MD simulations of a planar vesicle patch in a tensionless state, as done in MD studies of surfactant vesicles[30] and lipid membranes.[31] Also, simulations of a planar layer of *cis*-COSAN molecules could be relevant to understand the molecular ordering in the lyotropic lamellar phase obtained with H^+COSAN^- at high concentrations.[32] Preliminary results given in the Supporting Information indicate a local ordering (as measured by Co–Co correlation, see Figure S4) almost identical to that found inside the micelles. The organization of the molecules inside the layer shows a combination of two different molecular alignments with respect the assembly plane, in the attempt to maximize both contacts between molecules and orientation of hydrophilic regions towards the water phase (Figure S5).

In summary, we have demonstrated that the rich self-assembly behavior of cobaltabisdicarbollide (COSAN) anions can be interpreted from its molecular architecture based on a rotamer effect. According to our DFT implicit solvent calculations and in agreement with published crystal data, the most probable state in condensed phase (in water solution and in solid state) is the *cis*-COSAN rotamer. The molecular structure of this rotamer is such that it has well-defined hydrophilic and hydrophobic regions, as shown by our MD simulations. The hydrophobic region is an apolar region defined by the four carbon atoms of the molecule which are neighbors in the particular case of *cis*-COSAN. The boron atoms define a negatively charged region of the molecule that interacts strongly with water and thus forms the hydrophilic region of the molecule. In this molecular architecture, the *cis*-COSAN molecule is an amphiphilic molecule with a large hydrophilic region and a small hydrophobic one. Although most of the chemically synthetized surfactants have an opposite balance (i.e. a hydrophilic headgroup smaller than the hydrophobic tail) there are also many amphiphilic molecules with hydrophilic regions larger than the hydrophobic ones (most notably, biosurfactants[33] that also form micelles and vesicular structures). The results of our MD simulations reported here for *cis*-COSAN can be easily interpreted by considering this molecule as a classical amphiphilic molecule with a small hydrophobic "tail" defined by the four carbon atoms of the molecule and a large hydrophilic "head" defined by the boron atoms (see Figure 2c). As emphasized previously,[6] in many respects, the COSAN molecule experimentally behaves like a classical surfactant. Based on our calculations, we claim that the origin of this behavior is due to the architecture of the *cis*-COSAN molecule.

Acknowledgements

This work was supported by the Generalitat de Catalunya (grant 2017SGR1720) and the Spanish Ministry of Economy and Competitiveness through grants RTI2018-096273-B-I00, CTQ2016-75150-R and the "Severo Ochoa" Programme for Centres of Excellence in R&D (SEV-2015-0496) awarded to ICMAB. We thank the Spanish national supercomputing network (BSC-RES) for the award of computer time at the Minotauro supercomputer. D. C. Malaspina is supported by the European Union's Horizon 2020 research and innovation programme under Marie Sklodowska-Curie grant agreement No. 6655919.

Conflict of interest

The authors declare no conflict of interest.

Keywords: COSAN · molecular dynamics simulations · nano-ions · self-assembly

How to cite: *Angew. Chem. Int. Ed.* **2020**, *59*, 3088–3092
Angew. Chem. **2020**, *132*, 3112–3116

[1] K. Holmberg, B. Jönsson, B. Kronberg, B. Lindman, *Surfactants and Polymers in Aqueous Solution*, Wiley, Chichester, **2002**.
[2] J. N. Israelachvili in *Intermolecular And Surface Forces*, 3rd ed. (Ed.: J. N. Israelachvili), Academic Press, San Diego, **2011**, pp. 503–534.
[3] B. W. Ninham, P. Lo Nostro, *Molecular Forces and Self Assembly*, Cambridge University Press, Cambridge, **2010**.
[4] P. Bauduin, S. Prevost, P. Farràs, F. Teixidor, O. Diat, T. Zemb, *Angew. Chem. Int. Ed.* **2011**, *50*, 5298–5300; *Angew. Chem.* **2011**, *123*, 5410–5412.
[5] C. Viñas, M. Tarrés, P. González-Cardoso, P. Farràs, P. Bauduin, F. Teixidor, *Dalton Trans.* **2014**, *43*, 5062–5068.
[6] M. Uchman, V. Ďorďovič, Z. Tošner, P. Matějíček, *Angew. Chem.* **2015**, *127*, 14319–14323.
[7] R. Fernandez-Alvarez, V. Ďorďovič, M. Uchman, P. Matějíček, *Langmuir* **2018**, *34*, 3541–3554.
[8] V. Ďorďovič, Z. Tošner, M. Uchman, A. Zhigunov, M. Reza, J. Ruokolainen, G. Pramanik, P. Cígler, K. Kalíková, M. Gradzielski, et al., *Langmuir* **2016**, *32*, 6713–6722.
[9] R. Fernandez-Alvarez, Ž. Medoš, Z. Tošner, A. Zhigunov, M. Uchman, S. Hervø-Hansen, M. Lund, M. Bešter-Rogač, P. Matějíček, *Langmuir* **2018**, *34*, 14448–14457.
[10] M. Uchman, A. I. Abrikosov, M. Lepšík, M. Lund, P. Matějíček, *Adv. Theory Simulations* **2018**, *1*, 1700002.
[11] K. I. Assaf, W. M. Nau, *Angew. Chem. Int. Ed.* **2018**, *57*, 13968–13981; *Angew. Chem.* **2018**, *130*, 14164–14177.
[12] E. J. Juárez-Pérez, R. Núñez, C. Viñas, R. Sillanpää, F. Teixidor, *Eur. J. Inorg. Chem.* **2010**, 2385–2392.

[13] A. Zaulet, F. Teixidor, P. Bauduin, O. Diat, P. Hirva, A. Ofori, C. Viñas, *J. Organomet. Chem.* **2018**, *865*, 214 – 225.
[14] F. Teixidor, C. Viñas, *Pure Appl. Chem.* **2012**, *84*, 2457 – 2465.
[15] M. Bühl, D. Hnyk, J. Macháček, *Chem. Eur. J.* **2005**, *11*, 4109 – 4120.
[16] M. Bühl, J. Holub, D. Hnyk, J. Macháček, *Organometallics* **2006**, *25*, 2173 – 2181.
[17] M. J. Frisch, G. W. Trucks, H. B. Schlegel, G. E. Scuseria, M. A. Robb, J. R. Cheeseman, G. Scalmani, V. Barone, G. A. Petersson, H. Nakatsuji, et al., Inc., Wallingford CT, **2016**.
[18] W. J. Hehre, R. Ditchfield, J. A. Pople, *J. Chem. Phys.* **1972**, *56*, 2257 – 2261.
[19] V. A. Rassolov, J. A. Pople, M. A. Ratner, T. L. Windus, *J. Chem. Phys.* **1998**, *109*, 1223 – 1229.
[20] J. H. Jensen, *Molecular Modeling Basics*, CRC, Boca Raton, **2010**.
[21] J. Tomasi, B. Mennucci, R. Cammi, *Chem. Rev.* **2005**, *105*, 2999 – 3094.
[22] M. Cossi, V. Barone, R. Cammi, J. Tomasi, *Chem. Phys. Lett.* **1996**, *255*, 327 – 335.
[23] W. Humphrey, A. Dalke, K. Schulten, *J. Mol. Graph.* **1996**, *14*, 33 – 38.
[24] J. C. Phillips, R. Braun, W. Wang, J. Gumbart, E. Tajkhorshid, E. Villa, C. Chipot, R. D. Skeel, L. Kalé, K. Schulten, *J. Comput. Chem.* **2005**, *26*, 1781 – 1802.
[25] J. Huang, A. D. MacKerell, *J. Comput. Chem.* **2013**, *34*, 2135 – 2145.
[26] A. Pavlova, J. M. Parks, J. C. Gumbart, *J. Chem. Theory Comput.* **2018**, *14*, 784 – 798.
[27] M.-B. Sárosi, T. P. Lybrand, *J. Chem. Inf. Model.* **2018**, *58*, 1990 – 1999.
[28] S. Illa-Tuset, D. C. Malaspina, J. Faraudo, *Phys. Chem. Chem. Phys.* **2018**, *20*, 26422 – 26430.
[29] J. Hénin, G. Fiorin, C. Chipot, M. L. Klein, *J. Chem. Theory Comput.* **2010**, *6*, 35 – 47.
[30] L. Ferrer-Tasies, E. Moreno-Calvo, M. Cano-Sarabia, M. Aguilella-Arzo, A. Angelova, S. Lesieur, S. Ricart, J. Faraudo, N. Ventosa, J. Veciana, *Langmuir* **2013**, *29*, 6519 – 6528.
[31] S. Jo, J. B. Lim, J. B. Klauda, W. Im, *Biophys. J.* **2009**, *97*, 50 – 58.
[32] D. Brusselle, P. Bauduin, L. Girard, A. Zaulet, C. Viñas, F. Teixidor, I. Ly, O. Diat, *Angew. Chem. Int. Ed.* **2013**, *52*, 12114 – 12118; *Angew. Chem.* **2013**, *125*, 12336 – 12340.
[33] D. E. Otzen, *Biochim. Biophys. Acta Biomembr.* **2017**, *1859*, 639 – 649.

Manuscript received: October 16, 2019
Revised manuscript received: December 4, 2019
Accepted manuscript online: December 5, 2019
Version of record online: January 3, 2020

